ELSEVIER

Journal of Wind Engineering
and Industrial Aerodynamics 60 (1996) 195–209

JOURNAL OF wind engineering AND industrial aerodynamics

Experimental study of a plume in a crossflow

Eric Savory*, Norman Toy, Sarfraz Ahmed

Fluid Mechanics Research Group, Department of Civil Engineering, University of Surrey, Guildford GU2 5XH, UK

Abstract

The present work is an experimental wind tunnel study of the velocity field associated with a single turbulent jet or plume issuing through a circular nozzle flush with the ground plane and into a normal crossflow. The velocity data have been obtained by using a five-hole pressure probe which was operated in the nulled mode. From the flow vectors the vorticity distributions, the circulation associated with one of the dominant contrarotating vortices and the vortex doublet strength for the interaction have been determined. The data have been compared with both experimental and numerical turbulence model data from other workers. It was found that the development of the deflected jet was significantly dependent upon the initial boundary conditions in the flow field, in particular the jet boundary layer profile at the nozzle exit and the approach flow boundary layer along the ground plane.

Nomenclature

D	plume exit nozzle diameter
K	circulation associated with one vortex
U_p	plume exit velocity
$\tilde{U}$	crossflow velocity
U, V, W	longitudinal, lateral and vertical velocity components
V_m	magnitude of the velocity vector
X, Y, Z	longitudinal, lateral and vertical Cartesian axes
α	velocity ratio ($U_p/\tilde{U}$)
θ	pitch angle
μ	vortex doublet strength
ψ	yaw angle
ω_x	longitudinal vorticity component

* Corresponding author.

PII S0167-6105(96)00034-7

1. Introduction

The case of a single circular plume or jet issuing normally into a crossflow is a basic configuration with many engineering applications that has been extensively studied and reviewed [1–4]. The subject is of relevance to such diverse phenomena as ASTOVL aircraft, jet steering systems, combustion chamber mixing and sea outfall dispersion. In wind engineering such areas of interest include chimney or cooling tower dispersion, ventilation outlets and vehicle exhausts. The dominant features of the interaction are the formation of a pair of contrarotating vortices within the deflected plume and a turbulent wake flow. Although plume trajectories and nearby ground plane surface pressures can be determined with reasonable accuracy using established experimental data and prediction models there is very little experimental information available concerning the velocity field associated with the plume/crossflow interaction. The present work forms part of a wider fundamental study being undertaken by the authors [5–7] which encompasses both single and multiple plumes and jets issuing normally into a crossflow. This paper examines the velocity field associated with the vortex pair for three different plume velocity/crossflow velocity ratios (α), namely 4, 6 and 8. In each case the streamwise vorticity distribution, the total circulation associated with each vortex and the vortex doublet strength have been determined. The data have been compared with those obtained from turbulence model predictions, the preliminary results of which were presented in an earlier paper [5].

2. Experimental details

The experiments were carried out in a low-speed, blow-down wind tunnel which has working section dimensions of 1.37 m height × 1.07 m width × 9.0 m length and a free-stream turbulence level of 0.17%. The plume nozzle was located on the tunnel floor, at the midpoint of the 1.07 m section, approximately 4 m downstream of the tunnel contraction. The nozzle diameter was 28.5 mm and the exit was flush with the tunnel floor. The plumes were produced by a centrifugal fan connected to a simple pipe network manufactured from UPVC. Since the initial conditions are very important in the subsequent development of the plume/crossflow interaction, both the approaching boundary layer profile on the ground plane and the plume exit profiles were determined from hot-wire anemometer traverses. The ground plane boundary layer was developed naturally along working section floor. The main boundary layer parameters were; $\delta = 102$ mm (i.e. $3.58D$), $\delta_* = 18.6$ mm, $\theta = 13.6$ mm and $c_f = 0.00253$. Close to the ground plane the U-component turbulence level ($\sqrt{\overline{u^2}}/\tilde{U}$) was 8.7%. The plume exit velocity profiles were uniform over the central 80% of the diameter, whilst the turbulence level at the exit was approximately 0.8%.

The velocity measurements were carried out using a five-hole pressure probe and the device was employed in the nulled mode rather than in the fixed calibrated mode of the type suggested by Ref. [8]. It has been shown [9] that the nulled method of

operation is the most accurate since it minimises turbulence effects on the probe head by keeping the device aligned with the local mean flow direction. In the present work the movement of the probe was achieved by incorporating it into the end of a slender aerodynamic sting which formed part of a computer-controlled, stepper motor driven, five degree of freedom probe traversing mechanism (three translational axes and two rotational motions) located upon the roof of the wind tunnel. The pitch axis was a pantograph arrangement, whilst the probe yaw was achieved by rotating the entire angular axes mechanism about a vertical line through the probe tip. Hence, once the desired Cartesian position had been attained, the nulling of the probe side tube pressures was carried out by rotating the probe in pitch and yaw about the probe tip. The wind tunnel roof remained sealed throughout this operation by virtue of the fact that the roof section beneath the mechanism could traverse laterally and this section also included a longitudinal self-sealing slot through which the sting entered the tunnel. The roof and slot were also driven by stepper motors, activated by the movements of the sting. The pitch and yaw mechanisms were fitted with encoders to provide angular position data to $\pm 0.09°$ in pitch and $\pm 0.05°$ in yaw, whilst the positional accuracy of the Cartesian axes were maintained to within ± 0.02 mm. The probe tip diameter was 2.3 mm and the four outer holes were chamfered back at an angle of 45° (total included angle of 90°). The central pressure tube also had an internal chamfer at the tip in order to minimise the sensitivity of the total pressure measurement to changes in the local flow direction.

Pressure measurements were obtained using Furness differential transducers with ranges up to ± 25 mm water gauge. The measurement apparatus arrangement is illustrated diagrammatically in Fig. 1. The transducer output voltage caused by the

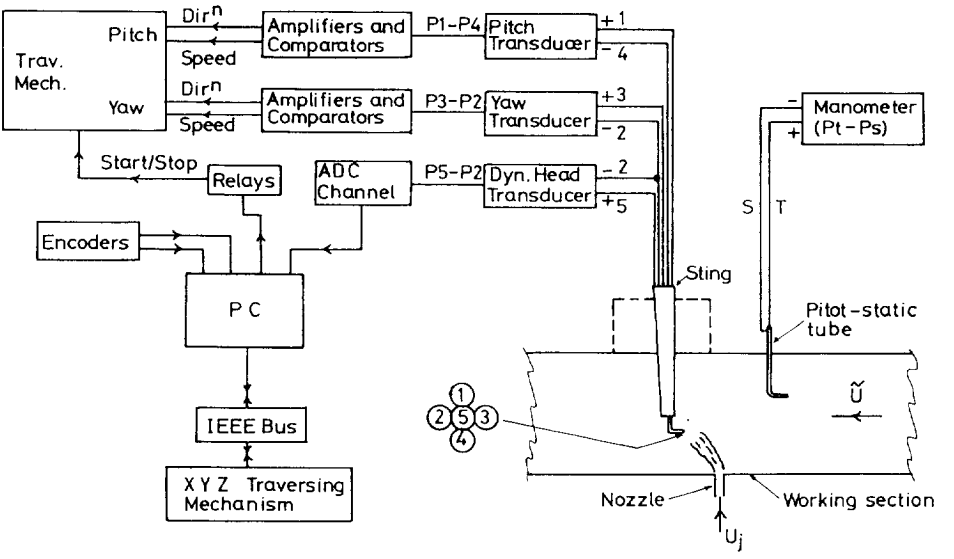

Fig. 1. Arrangement of experimental apparatus.

pressure difference between the upper and lower pitch tubes (P1 − P4) was used to control the movement of the pitch traversing mechanism so that the probe was moved towards alignment with the local mean flow direction (P1 = P4). This was achieved by utilising an amplifier and comparator arrangement in which the speed of the angular motion decreased as the null point was approached. The same traverse control arrangement was utilised to minimise the difference between the two yaw tubes (P3 − P2).

The velocity field data were derived from the measurements of the dynamic pressure (Pd) and the probe angles (θ, ψ). With the probe pressures nulled so that P1 = P4 (pitch) and P2 = P3 (yaw), the local dynamic pressure is given by

$$\mathrm{Pd} = k(\mathrm{P5} - \mathrm{P2}) = \tfrac{1}{2}\rho V_m^2,$$

where k is a constant (obtained by calibration against a pitot-static tube) and P5 is the total pressure measured in the central tube. From this data the three velocity vector components are

$$U = V_m \cos\theta \cos\psi, \quad V = V_m \cos\theta \sin\psi, \quad W = V_m \sin\theta.$$

The streamwise vorticity component (ω_x) was computed from the V and W velocity component distributions by first-order differencing. The total circulation associated with one of the pair of contrarotating vortices (K) was computed from the vorticity distributions by numerical integration using

$$K = \int\int \omega_x \, dY \, dZ.$$

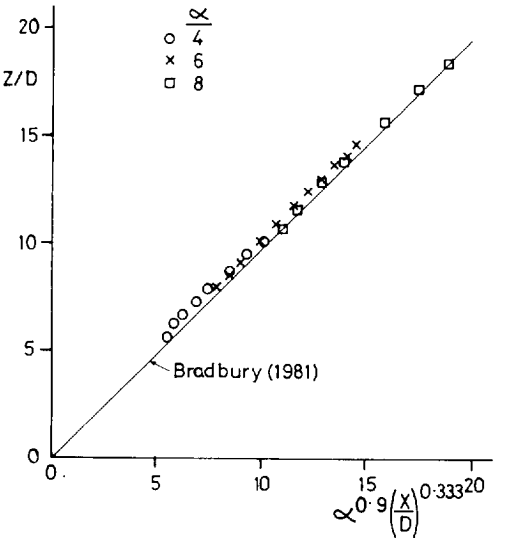

Fig. 2. Plume trajectories for the three velocity ratios.

The overall vortex doublet strength associated with this vorticity (μ) was computed in a similar manner

$$\mu = \int\int \omega_x Y \, dY \, dZ.$$

It has been shown that the vortex doublet strength is directly equivalent to a source-sink doublet when seen from the far-field [10,11]. From a conservative estimate of the experimental errors, incorporating uncertainties in measurement instrumentation, spatial positioning and numerical processing, the streamwise vorticity is within 10%, the circulation within 12% and the vortex doublet strength within 14%. During all of the experiments the crossflow velocity was 12 m/s, giving a Reynolds number of 2.3×10^4 based on nozzle diameter. The plume velocities were 48, 72 and 96 m/s, producing velocity ratios of 4, 6 and 8, respectively. In each case the velocity distributions in complete YZ planes were surveyed at locations between $X/D = 4$ and 25. An additional set of measurements were taken in a plane normal to the jet path, rather than in the Cartesian system, at $X/D = 8$ for $\alpha = 8$, in order to assess the effect of the reference frame of the measurements upon the integrated potential flow parameters.

3. Results and discussion

The plume trajectories, expressed as the locus of points of maximum total pressure measured on the centre-line at each downstream location, are illustrated in Fig. 2 for the three velocity ratios. It may be seen that there is good agreement with the prediction equation given in Ref. [2] which was derived from an assessment of the best existing data, that is

$$Z/D = 0.975 \, \alpha^{0.9} (X/D)^{0.333}.$$

The slightly greater, but consistent, plume penetration shown by the present data for a given velocity ratio and downstream location may be due to the presence of the thick ground plane boundary layer. Certainly, previous work has shown that the plume penetration increases with increasing thickness of the approach flow boundary layer. The extent of this effect was demonstrated in Ref. [12] from flow field measurements of pressure profiles for a plume with $\alpha = 1.96$ and two different boundary layer thicknesses of $\delta/D = 0.75$ and 2.25. Increasing the boundary layer thickness led to an increase of approximately 11% in the jet trajectory penetration at any given distance downstream of the nozzle. Clearly, the effect of the ground plane boundary layer will be greater for low velocity ratio plumes, such as that in Ref. [12], since the jet path will be located much nearer the wall. Some limited hot-wire anemometer velocity and turbulence measurements in the near wake of the jet by the present authors, with $\alpha = 6$ and for boundary layers of $\delta/D = 3.58$ and 9.1, confirmed the trend shown by Ref. [12]. The mechanisms by which the vorticity in the boundary layer is lifted upwards, as a result of the adverse pressure gradient, and entrained into the plume or jet on its leeward side have been observed from flow visualisation studies [13]. Hence,

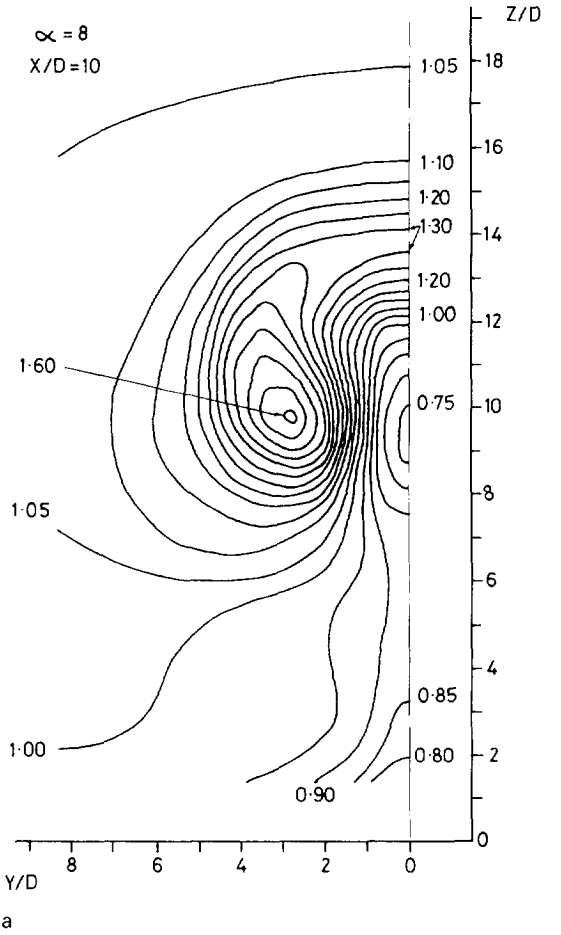

Fig. 3. Longitudinal velocity component in YZ planes at $X/D = 10$ and $X/D = 25$ for $\alpha = 8$: (a) $X/D = 10$; (b) $X/D = 25$.

it is evident that the contrarotating vortices in the deflected jet contain not only initial nozzle vorticity but also a significant proportion of ground plane boundary layer vorticity.

A representative set of velocity distributions for one-half of the plume are illustrated in Figs. 3 and 4, whilst Fig. 5 shows the corresponding longitudinal vorticity component distributions. Fig. 3 shows the longitudinal velocity component, normalised by the crossflow velocity, at two downstream YZ planes ($X/D = 10$ and $X/D = 25$) for $\alpha = 8$. The characteristic "kidney" shape associated with the deflected plume is very evident at both stations. In both cases the peak velocity within the plume is not located on the centre-line but within the lobes associated with the vortex. The projected velocity vectors in the same two YZ planes are shown in Fig. 4 where it may be seen that the

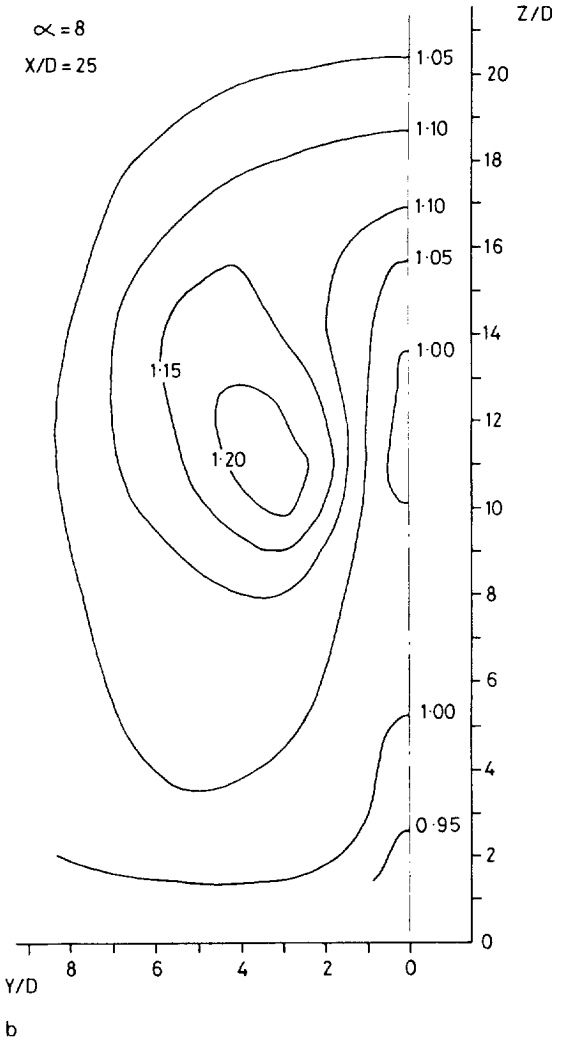

Fig. 3. Continued.

flow is entirely dominated by one of the contrarotating vortices. The associated distributions of longitudinal vorticity component, normalised as $\omega_x D/\tilde{U}$, are illustrated in Fig. 5. It may be seen that the peak vorticity value decreases with downstream distance as the plume expands, as would be expected. However, it has not been possible to produce a precise correlation of this peak vorticity data variation, between results from all three plume velocity cases, by simply using a function of α as the scaling parameter.

The variation with downstream distance of the total circulation associated with the vortex is shown in Fig. 6 for the three velocity ratios. The circulation is expressed in

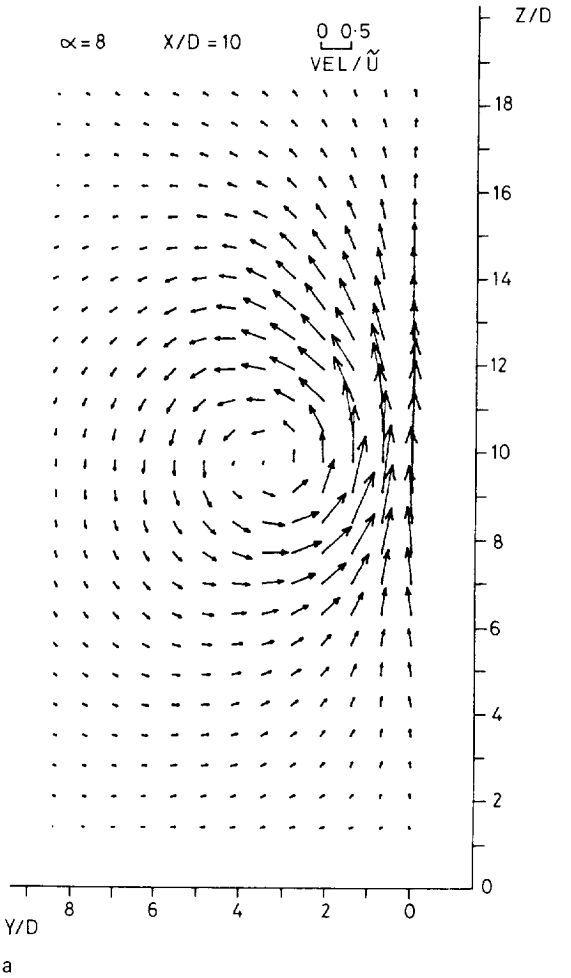

Fig. 4. Projected velocity vectors in YZ planes at $X/D = 10$ and $X/D = 25$ for $\alpha = 8$: (a) $X/D = 10$; (b) $X/D = 25$.

a non-dimensional form and the empirical relationship shown in the figure gives a reasonably good collapse of the data from the three different cases. It may be seen that the circulation builds up rapidly near the plume exit and then diminishes in the downstream direction due to the viscous diffusion associated with the interaction between the two vortices. At the nozzle exit the circulation may be considered to be approximately that derived from the freestream potential flow solution of the flow around a circular cylinder (the initial "solid" plume), which gives $K/D\tilde{U} = 2$, [3,11]. From analysis of the momentum balance far downstream [3] it has been shown that for large velocity ratios the circulation will tend towards $K/D\tilde{U} = 6$. Certainly, the present data for the highest velocity ratio, $\alpha = 8$, tend towards this value, giving

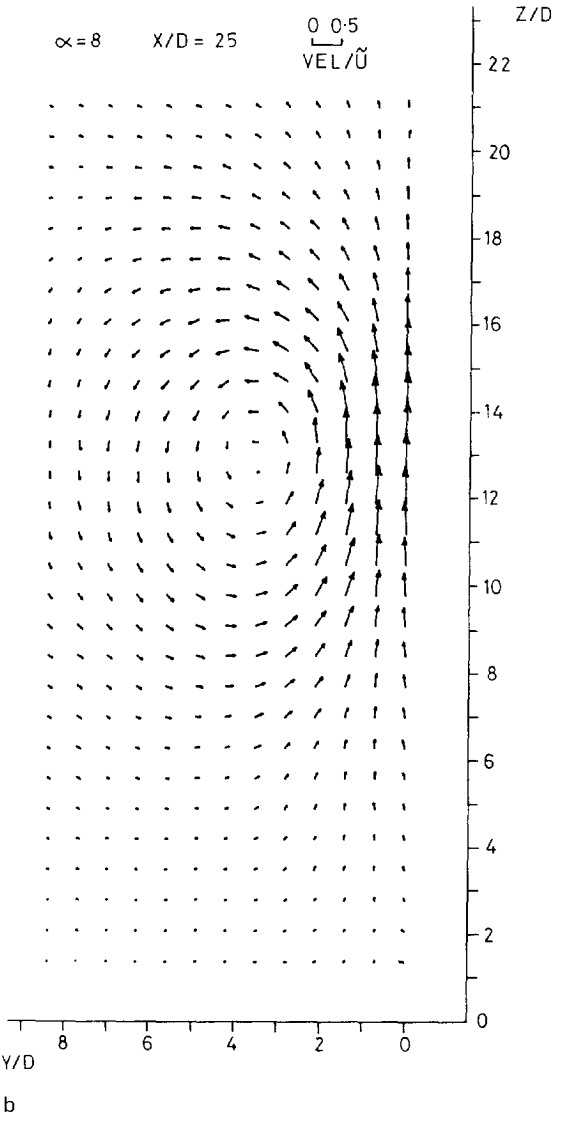

Fig. 4. Continued.

$K/D\tilde{U} = 7.1$ at $X/D = 25$. The diamond symbol in the figure, at $X/D = 8$, shows the result obtained from the plume path plane of measurements which agrees well with the main sets of data.

The results from other workers are shown, superimposed on the present data, in Fig. 7. The experimental data of Thompson [11] was obtained at a similar Reynolds number to that in the present work, with the main difference being that in Ref. [11] the

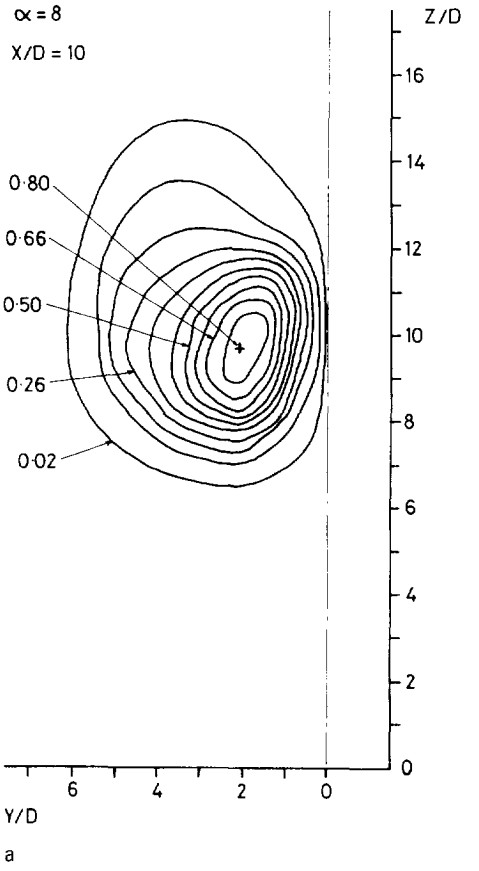

Fig. 5. Longitudinal vorticity component in YZ planes at $X/D = 10$ and $X/D = 25$ for $\alpha = 8$: (a) $X/D = 10$; (b) $X/D = 25$.

ground plane boundary layer was almost entirely removed by suction upstream of the nozzle. Most of the data obtained in Ref. [11] was achieved by using a manually nulled five-hole pressure probe but in almost all cases the total circulation and vortex doublet strength were estimated from the results obtained from a single vertical traverse through the vortex centre. This required the somewhat erroneous assumptions that each vortex was circular and that there was no interaction between the vortex pair. There appears to be reasonable agreement between the present data and that of Ref. [11] for the lowest velocity ratio ($\alpha = 2.3$) but not for the highest velocity ratio ($\alpha = 8.1$). However, the general trend of a decrease in circulation with downstream distance from the nozzle exits is evident in all of the data from Ref. [11]. The turbulence model predictions by Sakellariou [14] utilised the same boundary conditions adopted in the present work. The results shown in Fig. 7 are from a Reynolds stress transport model using a grid of 58 000 points. The model used the QUICK

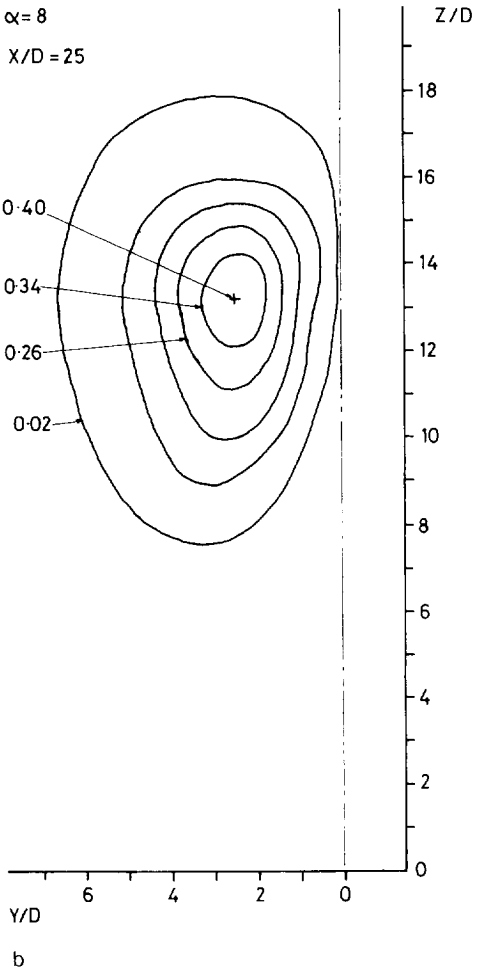

Fig. 5. Continued.

algorithm to provide second-order accurate discretisation in the momentum equations, which was essential for any realistic predictions to be carried out, and SMART to ensure boundedness at all stages during the iteration process. This arrangement gave the best agreement with the present data, with the general trend for the circulation being well predicted although the magnitude of the circulation is rather high. The k–ε model with QUICK differencing produced a similar trend (not shown in the figure) but with circulation values some 50% higher than those obtained from the Reynolds stress model. This was attributed to the inability of the k–ε model to reproduce the extent of the diffusion of the longitudinal vorticity, which resulted in prediction of a smaller, much tighter vortex with its centre nearer the centre-line than in the experiments. As a result the total circulation was grossly over-predicted. The

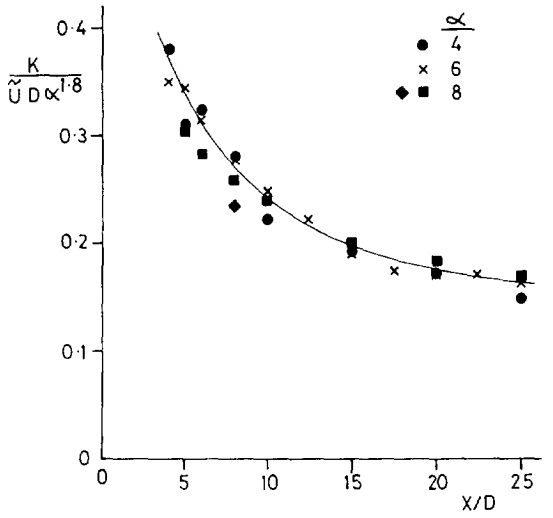

Fig. 6. Variation of circulation with downstream distance for the three velocity ratios.

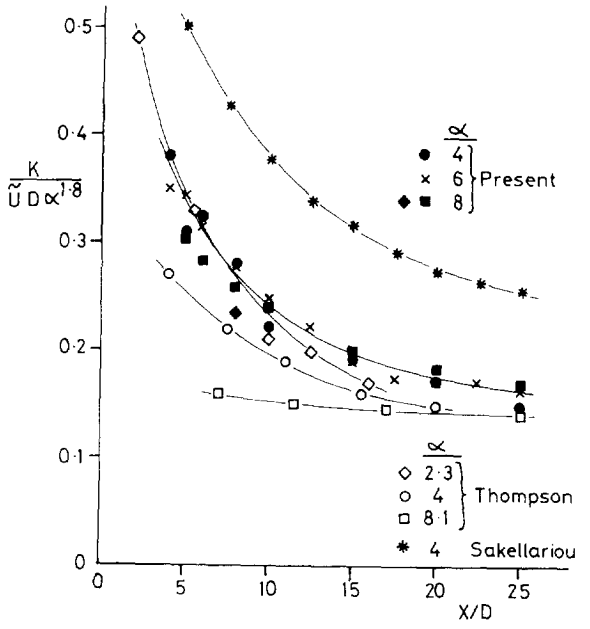

Fig. 7. Comparison of variation of circulation with other workers.

work carried out in Ref. [14] also highlighted the importance of accurately modelling the initial conditions if reasonable agreement with the experimental data is to be achieved. The earlier calculations, which did not model either the ground plane boundary layer or the nozzle exit boundary layer, produced very poor agreement with

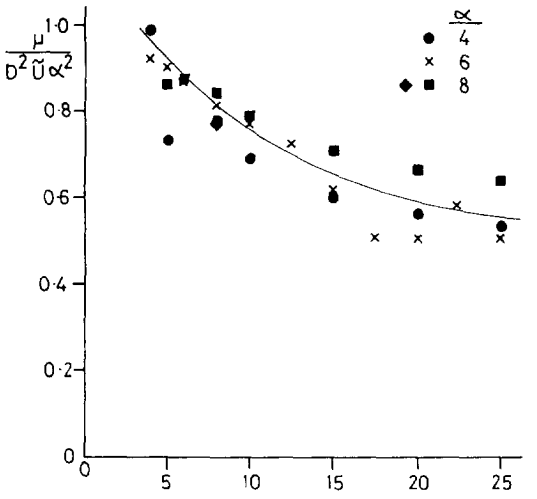

Fig. 8. Variation of vortex doublet strength with downstream distance for the three velocity ratios.

the present data. Hence, when carrying out such plume/crossflow calculations sufficient grid nodes must be provided in the nozzle exit region in order to accurately capture the initial vorticity distributions.

The variation of the vortex doublet strength with distance from the exit is shown in Fig. 8, with the data normalised by the initial plume momentum flux. Although there is some scatter in the data the results from the three cases collapse reasonably well. Far downstream the plume is almost horizontal and so the lift force acting on it may be considered to be the same as a three-dimensional body in potential flow, that is $\rho\mu\tilde{U}$ [2]. Neglecting the ground plane forces, this force may be approximately equated to the initial plume momentum flux which, taking into account the reduction effect of the nozzle boundary layer, gives an asymptotic value for Fig. 8 of 0.66. This result shows reasonable agreement with the present data. At the nozzle exit the vortex doublet strength may be approximated by considering that the plume is represented by circular "cylinder" in the XY plane with two-dimensional potential flow provided by the crossflow. This yields the initial exit value of π/D for the normalised vortex doublet strength $\mu/\tilde{U}D^2$, which is independent of velocity ratio α. This initial small value for μ indicates that the vortex doublet strength must build up very rapidly within the first few diameters from the jet exit. The diamond symbol shown at $X/D = 8$ represents the result from the plane of measurements taken normal to the jet path and, again, there is good agreement with the other data sets.

The vortex doublet strength data is shown, together with the present work, in Fig. 9. The continual decrease in vortex doublet strength with downstream distance, beyond $X/D = 4$ shown by the present work, is in agreement with the turbulence model predictions of Sakellariou [14] and some data from high speed jet flows Galliard et al. [15] obtained from Cartesian grid velocity measurements taken using laser Doppler anemometry. The numerical calculations [14] tend to underestimate

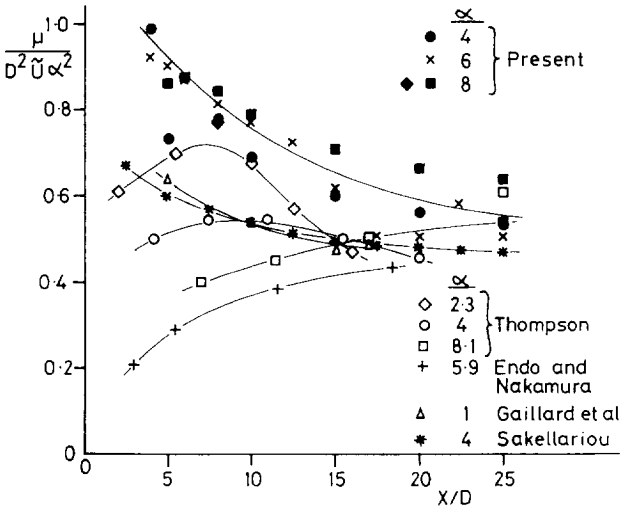

Fig. 9. Comparison of variation of vortex doublet strength with other workers.

the vortex doublet strength throughout the downstream distance covered. This is because, although the peak vorticity value is well-predicted by the Reynolds stress model and the total circulation is over-predicted, the lateral diffusion of the vorticity, which produces the moment, is much less than in the experiment. The data from Ref. [11] tends to contradict the present work in that the vortex doublet strength increases with downstream distance for the higher velocity ratio. However, the asymptotic value far downstream agrees well with the present work. The results of Endo and Nakamura [16] also show differences from the present work in the near-exit region. However, it should be noted that the experimental configuration in Ref. [16] the plume exited through a chimney-like nozzle which protruded some $6.5D$ through the ground plane into the crossflow. Hence, the flow in the near-exit region was complicated by the highly three-dimensional flow around the top of the cylindrical nozzle, thereby making comparisons with other data rather tenuous. In addition, the vorticity distributions in Ref. [16] were very distorted and not symmetrical about the centreline, casting doubt upon the flow quality within the wind tunnel and plume rig. Nevertheless, the asymptotic value of μ is similar to that in the present work.

4. Concluding remarks

The data obtained from the plume/crossflow interaction show that far downstream from the exit the main parameter influencing the potential flow quantities (circulation and vortex doublet strength) is the velocity ratio. However, the initial distribution of vorticity (in the ground plane boundary layer and in the plume nozzle) also plays a very important role in the subsequent development of the deflected plume. In

addition, comparisons with numerical turbulence model computations show that the lateral diffusion of vorticity is poorly predicted with a k–ε model. However, a Reynolds stress transport model, together with QUICK differencing, reproduces the peak vorticity very well and the overall vortex doublet strength to an acceptable degree, particularly in the region well downstream of the nozzle.

Acknowledgements

The present work was supported by the UK Ministry of Defence with DRA Farnborough. The authors are indebted to Mr. P.B. Earnshaw for his constant support and guidance throughout the research. We are also grateful to Professor J.J. McGuirk and Dr. N. Sakellariou of Loughborough University for permission to utilise their c.f.d. data in this research work.

References

[1] E.C.P. Ransom and P.M. Wood, Jet interference literature survey and critical review, Kingston Polytechnic Report 75/1/ER (1974).
[2] L.J.S. Bradbury, Some aspects of jet dynamics and their implications for VTOL research in: Proc. N.A.T.O. A.G.A.R.D. Conf. CP-308, 1981, pp. 1.1–1.2.
[3] G.J. Hancock, A review of the aerodynamics of a jet in a cross flow, Aeronautical J. 91 (1987) 201.
[4] R.J. Margason, Fifty years of jet in crossflow research, in: Proc. N.A.T.O. A.G.A.R.D. Conf. CP-534, 1993, pp 1.1–1.4.
[5] E. Savory, N. Toy, J.J. McGuirk and N. Sakellariou, An experimental and numerical study of the velocity field associated with a jet in a crossflow, in: Proc. Int. Symp. on Engineering Turbulence Modelling and Measurements, Dubrovnic, 1990, pp. 165–174.
[6] E. Savory and N. Toy, Real-time video analysis of twin jets in a cross flow, ASME J. Fluids Eng. 113 (1991) 68.
[7] N. Toy, E. Savory, S. McCusker and P.J. Disimile, The interaction region associated with twin jets and a normal crossflow, in: Proc. N.A.T.O. A.G.A.R.D. Conf. CP-534, 1993, pp. 7.1–7.10.
[8] A.L. Treaster and A.M. Yocum, The calibration and application of five-hole probes, ISA Trans. 18 (1978) 23.
[9] T. Christiansen and P. Bradshaw, Effect of turbulence on pressure probes, J. Phys. E 14 (1981) 992.
[10] P.E. Rubbert, Calculation of jet interference effects on V/STOL aircraft by nonplanar potential flow method, in: Proc. N.A.S.A. SP-218, 1969, pp. 181–204.
[11] A.M. Thompson, The flow induced by jets exhausting normally from a plane wall into an airstream, Ph.D. Thesis, University of London (1971).
[12] Y. Sugiyama and M. Kawase, A flow field with a jet affected by a uniform crossflow, Bull. Japan Soc. Mech. Eng. 28 (1985) 1387.
[13] T.F. Fric and A. Roshko, Structure in the near field of the transverse jet, in: Proc. 7th Symp. on Turbulent Shear Flows, Stanford University, USA, 1989, 6.4.1–6.4.6.
[14] N. Sakellariou, Numerical predictions of jet in cross-flow aerodynamics, Ph.D. Thesis, Imperial College London (1993).
[15] R. Gaillard, D. Geffroy, L. Jacquin and G. Losfeld, Etude experimentale sur les interactions antre un jet supersonique chauffe transversal et un ecoulement supersonique externe, in: Proc. N.A.T.O. A.G.A.R.D. Conf. CP-534, 1993, pp. 39.1–39.10.
[16] H. Endo and M. Nakamura, Bending and development of three-dimensional turbulent jets in a crosswind, Nat. Aerospace Lab. (Japan), Report TR-216 (1970).